analytical chemistry

pubs.acs.org/ac Article

Glutamate Electropolymerization on Carbon Increases Analytical Sensitivity to Dopamine and Serotonin: An Auspicious *In Vivo* Phenomenon in Mice?

Jordan Holmes, Colby E. Witt, Deanna Keen, Anna Marie Buchanan, Lauren Batey, Melinda Hersey, and Parastoo Hashemi*

Cite This: *Anal. Chem.* 2021, 93, 10762−10771 Read Online

ACCESS | Metrics & More | Article Recommendations | Supporting Information

ABSTRACT: Carbon is the material of choice for electroanalysis of biological systems, being particularly applicable to neurotransmitter analysis as carbon fiber microelectrodes (CFMs). CFMs are most often applied to dopamine detection; however, the scope of CFM analysis has rapidly expanded over the last decade with our laboratory's focus being on improving serotonin detection at CFMs, which we achieved in the past *via* Nafion modification. We began this present work by seeking to optimize this modification to gain increased analytical sensitivity toward serotonin under the assumption that exposure of bare carbon to the *in vivo* environment rapidly deteriorates analytical performance. However, we were unable to experimentally verify this assumption and found that electrodes that had been exposed to the *in vivo* environment were more sensitive to evoked and ambient dopamine. We hypothesized that high *in vivo* concentrations of ambient extracellular glutamate could polymerize with a negative charge onto CFMs and facilitate response to dopamine. We verified this polymerization electrochemically and characterized the mechanisms of deposition with micro- and nano-imaging. Importantly, we identified that the application of 1.3 V as a positive upper waveform limit is a crucial factor for facilitating glutamate polymerization, thus improving analytical performance. Critically, information gained from these dopamine studies were extended to an *in vivo* environment where a 2-fold increase in sensitivity to evoked serotonin was achieved. Thus, we present here the novel finding that innate aspects of the *in vivo* environment are auspicious for detection of dopamine and serotonin at carbon fibers, offering a solution to our goal of an improved fast-scan cyclic voltammetry serotonin detection paradigm.

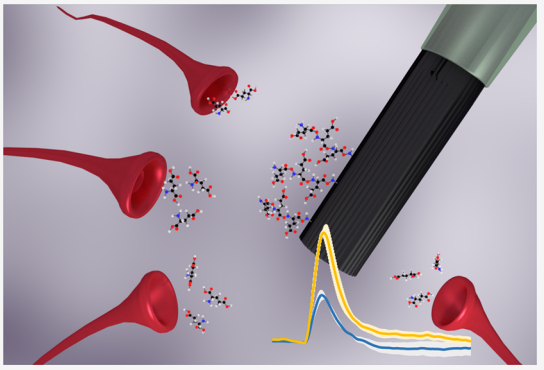

INTRODUCTION

Carbon electrodes are uniquely amenable for biological analyses, in particular detection of neurochemicals in dynamic and complex media. The carbon surface is biocompatible and versatile (easily fashionable into multiple configurations); a variety of available carbon forms provide an extensive catalogue of electroanalytical opportunities.[1−4] Within neurochemical analysis with this material, carbon fiber microelectrodes (CFMs) are particularly popular.[5,6] For several decades, fast-scan cyclic voltammetry (FSCV) at CFMs has been employed to study dopamine in the context of pathologies such as addiction and Parkinson's disease.[7−9] In tandem to this work, the electrochemical properties governing the FSCV response toward dopamine have been well explored, including the regenerative ability of carbon, electron transfer kinetics, and adsorption interactions at the carbon fiber surface interface.[10−14]

In the last decade, the scope of FSCV has been expanded to analytes other than dopamine.[15−20] In our laboratory, we pioneered FSCV for serotonin and applied these measurements *in vivo*.[21,22] We have used the method over the last 10 years to investigate serotonin dynamics in a variety of *in vivo* scenarios including probing neurochemistry between sexes, analyzing the effects of antidepressants, investigating mouse models of disease, and mapping the biochemical architecture in different brain regions.[23−27] However, serotonin detection with CFMs remains niche because serotonin signaling is highly regulated *in vivo*, with very low evocable concentrations (low nM range compared to 10 μM evoked dopamine).[28] Furthermore, the primary serotonin metabolite, 5-hydroxyindole acetic acid (5-HIAA), rapidly electropolymerizes on the electrode surface and reduces the *in vivo* signal re-

Received: October 13, 2020
Accepted: June 3, 2021
Published: July 30, 2021

https://doi.org/10.1021/acs.analchem.0c04316
Anal. Chem. 2021, 93, 10762−10771

sponse.[22,29−31] Our approach to facilitating serotonin detection has been to modify the electrode surface *a priori* with Nafion, a sulfonated tetrafluoroethylene-based cation exchange polymer, that preconcentrates serotonin and repels 5-HIAA.[22]

There has, in recent years, been incongruity in the community about an optimal Nafion modification procedure,[31−35] and there have been reports of alternative polymer modifications (such as poly(3,4-ethylenedioxythiophene) (PEDOT)).[36−38] Thus, we sought to further improve FSCV's sensitivity toward serotonin by optimizing a Nafion modification protocol that would facilitate broader adoption of the method. However, before we could assess the effects of the polymer coating, we encountered an unusual phenomenon. Specifically, we were unable to replicate a key assumption in the field—that sensitivity toward monoaminergic cations decreases after electrode implantation into brain tissue.[29,31] We found that after *in vivo* implantation, electrodes were significantly *more* sensitive to dopamine using both FSCV and fast-scan controlled-adsorption voltammetry (FSCAV). The rationale that electrodes should be less sensitive to dopamine after *in vivo* implantation is that polymerization of proteins and metabolites (such as 5-HIAA) makes the surface less accessible to dopamine. Using the same rationale, we considered which brain chemicals had the potential to interact with the electrode creating a positive effect for dopamine detection. Glutamate is a ubiquitous neurotransmitter, present at high concentrations throughout the brain. This amino acid has been shown previously to electropolymerize, forming polyglutamic acid (PGA) on carbon surfaces, *via* a radical-initiated mechanism.[39−42] PGA possesses an overall negative charge at biological pH; thus, we postulated that a PGA coating on CFMs might improve sensitivity toward dopamine. Indeed, we found that electrodes electrochemically pretreated in glutamate solution displayed significantly better analytical responses to dopamine *via* flow injection analysis (FIA). We showed electrochemical evidence for glutamate polymerization onto CFMs and characterized this film *via* scanning electron microscopy (SEM) and atomic force microscopy (AFM). We found that PGA films serve to stabilize or replace Nafion films with prolonged (>2 h) use, an opportune outcome of the *in vivo* environment that facilitates measurements. Finally, we exploited this finding to make a minor modification to our serotonin detection waveform that resulted in a 2-fold increase in response amplitude toward serotonin in the CA2 region of the hippocampus.

Given the analytical and morphological similarities between *in vivo* and PGA electrodes, we conclude that the high levels of ambient brain glutamate play a role in enhancing *in vivo* CFM measurements in the mouse brain. Using this finding, we present a novel treatment protocol to improve the sensitivity of FSCV toward serotonin *in vivo*, which was the original goal of this study. Importantly, this work allows us to suggest that carbon's suitability for neurochemical electroanalysis includes an innate and auspicious interaction of amino acids, like glutamate, with this substrate.

EXPERIMENTAL SECTION

General Methods and Materials. *Chemicals.* Stock solutions were prepared at room temperature and physiological pH (pH = 7.4) by dissolving glutamic acid and dopamine hydrochloride (each prepared to a final concentration of 1 μM) into 1× phosphate buffered saline (PBS) that was diluted from a 10× premixed buffer. Serotonin hydrochloride was prepared similarly in TRIS hydrocholoride buffer, as described elsewhere.[22,26] All chemicals were purchased from Sigma Aldrich (St. Louis, MO) unless otherwise specified. Liquion (LQ-1105, 5% by weight Nafion) was purchased from Ion Power Solutions (New Castle, DE, USA).

Electrochemistry. Voltammetry was performed on a two-electrode system. CFMs were handmade in-house as previously described.[25] Briefly, a single carbon fiber (*d*iameter = 7 μm; Goodfellow Corporation, PA, USA) was aspirated into a glass capillary (1.0 mm external diameter, 0.5 mm internal diameter, A-M Systems, Inc., Sequim, WA, USA). The glass capillary was then pulled with a vertical micropipette puller (Narishige, Tokyo, Japan) to form a carbon-glass seal. The exposed length of the carbon fiber was trimmed to 100 μm under an optical microscope. A Ag wire (A-M systems, WA, USA) was electroplated with Cl^- for 30 s in 0.1 M HCl at 5 V to create a pseudo-Ag/AgCl reference electrode.

Fast-Scan Cyclic Voltammetry (FSCV). Waveforms were generated using a USB-6431DAC/ADC (National Instruments, TX, USA) device. The working electrode was controlled with a waveform (details on waveforms are specific to each experiment, see below). The electrode was cycled at 60 Hz for 10 min and then at 10 Hz for 10 min. This dual frequency strategy speeds up surface preparation but can be achieved with 10 Hz applied for longer.

Fast-Scan Controlled-Adsorption Voltammetry (FSCAV). FSCAV was performed as previously described[43,44] using a CMOS precision analog switch, ADG419 (Analog Devices), to control the application of the waveform. The waveform (DA: −0.4 V to +1.3 V to -0.4 V, scan rate = 1200 V/s) was applied at a frequency of 100 Hz for 2 s and then held at a constant potential of −0.4 V for 10 s followed by reapplication of the waveform for the remainder of the total file collection time of 30 s. Cyclic voltammograms (CVs) were used for DA identification. With FSCAV, the first CV after reapplication of the waveform with a signature DA peak was integrated to determine charge.

Flow Injection Analysis (FIA). FIA was performed in a system, custom-built in-house. CFMs were inserted into a flangeless short, 1/8 nut (PEEK P-335, IDEX, Middleboro, MA, USA), exposing a small portion of the tip (2 mm) outside of the nut. An HPLC union (Elbow PEEK 3432, IDEX, Middleboro, MA, USA) was modified such that the nut containing the microelectrode was fastened to one end. The out-flowing stream of the FIA buffer was fastened to the other end of the elbow union. Two holes were drilled into the union for the incorporation of the pseudo-Ag/AgCl reference electrode and the "waste" flow stream. A syringe infusion pump (KD Scientific, Model KDS-410, Holliston, MA, USA) was used to maintain the flow at 2 mL min^{-1}. The analyte was introduced into the flow stream for 10 s *via* a six-port HPLC loop injector (Cheminert Valve, VICI, Houston, TX, USA) resulting in a rectangular plug.

Data Acquisition. FSCV and FSCAV were performed using a Dagan potentiostat, (Dagan Corporation, Minneapolis, MN, USA), National Instruments multifunction IO device USB-6341 (National Instruments, Austin, TX, USA), WCCV 3.06 software (Knowmad Technologies LLC, Tucson, AZ, USA), and a Pine Research head stage (Pine Research Instrumentation, Durham, NC, USA). Data filtering (zero phase, Butterworth, 2 kHz low-pass) and signal smoothing were performed within the WCCV software.

https://doi.org/10.1021/acs.analchem.0c04316
Anal. Chem. 2021, 93, 10762−10771

Nafion Electrodeposition. Nafion was electrodeposited on the exposed carbon fiber surface by applying a constant potential of 1.0 V vs. a pseudo-Ag/AgCl reference electrodefor 30 s. The microelectrode was dried at 70 °C for 10 min and stored for a minimum of 24 h before use.

Animals. Animal use followed NIH guidelines and complied with the University of South Carolina Institutional Animal Care and Use Committee under an approved protocol. *In vivo* animal experiments were performed as described previously.[24] To induce anesthesia, 25% w/v urethane (Sigma−Aldrich Co.) dissolved in 0.9% NaCl solution (Hospira) was injected i.p. (7 μL g^{-1} of body weight). Body temperature was maintained using a heating pad (Braintree Scientific, Braintree, MA, USA), and stereotaxic surgeries (David Kopf Instruments, Tujunga, CA, USA) were performed with coordinates taken in reference to bregma. Specific coordinates used in each experiment can be found below under "Specific Methods." A pseudo-Ag/AgCl reference electrode was placed in the contralateral hemisphere.

Specific Methods. *Figure 1.* Four-point pre-calibrations were performed before *in vivo* experiments, and post-calibrations were performed within 12 h after *in vivo* experiments where charge (pC for FSCAV measurements) or current (nA for FSCV measurements) was plotted vs. [DA] (nM). If the electrodes were left overnight, they were stored dry in a box at constant temperature. Nafion-coated CFMs were placed in target regions of the mouse brain for *in vivo* exposure times of 2 h, typical of an *in vivo* experiment. For FSCAV data, a Nafion-coated CFM was lowered into the nucleus accumbens core region of the brain (AP: +0.8, ML: +1.3, DV -4.0). CFMs trimmed to 50 μm were cycled using the modified waveform described above. For FSCV data, a CFM was lowered until it was fully immersed in the dorsal striatum (AP: +1.1, ML: +1.7 DV: −2.0) and a triangular waveform was applied (−0.4 V to 1.3 V to −0.4 V, scan rate = 400 V/s) for 10 min at 60 Hz and 10 min at 10 Hz. Dopamine release was electrically evoked *via* MFB stimulation (AP: -1.8, ML: +1.1, DV: -4.8). All data were averaged over at least eight electrodes, and the standard error of the mean was calculated (represented by error bars). A one-tailed paired *t*-test was utilized to determine the significance between two points ($p < 0.05$).

Figure 2. The current amplitude and electrode temporal response of various combinations of CFM pretreatments for dopamine analysis with FIA were compared. Dopamine analysis was performed using FSCV with the following triangular waveform: −0.4 V to 1.3 V to −0.4 V at 400 V/s. Each modification protocol was evaluated by averaging the response of five injections of 1 μM dopamine on four electrodes in the bar graph. Additionally, the first 3.5 s of the FIA pulse associated with a dopamine injection is displayed and the slope was calculated by isolating the linear region of the rise curve.

The modification protocols tested were as follows:

1. Bare: unmodified CFM serving as a control.
2. Glu: glutamate pretreatment and glutamate in FIA calibration buffer. To deposit PGA, CFMs were dipped in 1 μM glutamate solution (in 1× PBS buffer) and cycled using the same triangular waveform (−0.4 V to 1.3 V to −0.4 V, 400 V/s) applied during analysis for 10 min at 60 Hz and 10 min at 10 Hz.
3. *In Vivo*: *in vivo* pretreatment. Electrodes were placed into the cortex of a rodent brain (AP: +0.8, ML: +1.7, DV -0.5) for 20 min and dopamine was measured immediately thereafter with FIA in PBS only.
4. *In Vivo* + Glu: *in vivo* pretreatment and glutamate in FIA calibration buffer. Electrodes underwent the *in vivo* pretreatment as in (3) above and 1 μM glutamate was added to the FIA buffer.

Figure 3. Glutamate electropolymerization events were captured on CFMs trimmed to 100 μm using a waveform with a wide potential window: −1.2 V to 1.3 V to −1.2 V at 400 V/s. With FIA, data from 30 glutamate injections at 0.1 μM were collected followed by 10 injections each of 1, 20, and 100 μM. The peak at 1 V was quantified as the glutamate electropolymerization event, and the responses of four electrodes were averaged. Error bars were calculated using standard error the mean.

Scanning Electron Microscopy (SEM). Electrodes were prepared for SEM imaging by depositing PGA, employing two triangular waveforms: (1) −0.4 V to 1.3 V to −0.4 V and (2) −0.4 V to 1.0 V to −0.4 V; each at 400 V/s. Electrodes were then transported to the microscope in a closed container. The capillary glass was cracked, and the tip end of the CFM was secured onto a stage with double-sided tape. SEM images were collected using a Zeiss Ultraplus thermal field emission scanning electron microscope. Images in Figure 3Bi−iii were magnified on the Zeiss software, and the image in Figure 3Biv was digitally magnified. The edge planes were imaged because significant electrochemistry happens on this plane. The CFM modifications imaged are listed below:

1. PBS, 1.3 V: CFMs were cycled for 20 min total (60 Hz 10 min, 10 Hz 10 min) using triangular waveform 1, with a positive potential limit of 1.3 V, in PBS.
2. Glutamate in PBS, 1.0 V: CFMs were cycled for 20 min total (60 Hz 10 min, 10 Hz 10 min) using triangular waveform 2, with a positive potential limit of 1.0 V, in 10 mM glutamate.
3. Glutamate in PBS, 1.3 V: CFMs were cycled for 20 min total (60 Hz 10 min, 10 Hz 10 min) using triangular waveform 1, with a positive potential limit of 1.3 V, in 10 mM glutamate.
4. *In Vivo*, 1.3 V: The electrode was placed into the cortex of a rodent brain (AP: +0.8, ML: +1.7, DV: -0.5) and cycled for approximately 20 min total (60 Hz 10 min, 10 Hz 10 min) with triangular waveform 1, with a positive potential limit of up to 1.3 V.

Dopamine Analysis. 1 μM DA was measured using FIA either in the presence or absence of 1 μM glutamate within the running buffer (1× PBS). CFMs were cycled for 20 min total (60 Hz 10 min, 10 Hz 10 min) prior to analysis, and the current response of four CFMs was measured using the triangular waveform: −0.4 V to 1.0 V to −0.4 V at 400 V/s. Cycling was then repeated immediately using a slightly modified triangular waveform: −0.4 V to 1.3 V to −0.4 V at 400 V/s, and the current response of the same four electrodes was reanalyzed. A *t*-test was used to determine statistical significance.

Atomic Force Microscopy (AFM). Electrodes were prepared for AFM imaging by depositing PGA or Nafion on the day of analysis. Electrodes were transported to the AFM in a closed container and mounted on a glass slide, with the electrode tip flat to the slide surface. AFM images were collected using a Digital Instruments Dimension 3100 AFM (Veeco Metrology Group) with a NanoScope IIIa Controller and a non-contact

https://doi.org/10.1021/acs.analchem.0c04316
Anal. Chem. 2021, 93, 10762−10771

tip. In Figure 3Ci−iii, CFMs were imaged immediately following pretreatment. Treatments include (i) cycling a bare electrode in PBS buffer for 20 min (10 min 60 Hz, 10 min 10 Hz), (ii) electroplating Nafion (method described above), and (iii) electropolymerizing PGA with triangular waveform (−0.4 V to 1.3 V to −0.4 V, scan rate of 400 V/s) by cycling for 20 min (10 min 60 Hz, 10 min 10 Hz) in PBS buffer containing 1 μM glutamate. In Figure 3Civ-v, CFMs were cycled (10 Hz) for 2 h with a triangular waveform (−0.4 V to 1.3 V to −0.4 V, scan rate of 400 V/s) before imaging, to simulate the length of a typical *in vivo* experiment. Treatments include (iv) Nafion electroplating and (v) electropolymerizing PGA on Nafion-coated CFMs using the same procedure as (iii) prior to cycling.

Figure 4. The "Jackson" waveform was employed to measure serotonin (0.2 V to −0.1 V to 1.0 V to 0.2 V, scan rate: 1000 V/s). In Figure 4A, 100 nM serotonin was measured in the presence of 10 μM 5-HIAA in TRIS buffer on electrodes trimmed to 150 μm.

Measurements were collected with FIA every 30 min for 2 h. The serotonin oxidation peak at 0.7 V was quantified, and the current response of three or four electrodes was averaged. Error bars were calculated using standard error of the mean. CFMs that underwent an electrochemical activation pretreatment were cycled using a modified "Jackson" waveform where the positive potential limit was raised to 1.3 V for 10 min at 60 Hz and 10 min at 10 Hz. The electrodes were then cycled again, and analysis was performed using the original "Jackson" waveform (positive potential limit of 1.0 V) . In Figure 4B, a CFM trimmed to 150 μm was placed into the CA2 region of the mouse hippocampus (AP: −2.91 ML: +3.35 DV: −2.5). Serotonin was evoked *via* electrical stimulation to the MFB (coordinates above), and data was collected and average from four animals for the Jackson waveform (black) and the same after a 10 min treatment period with the extended Jackson waveform (yellow). The maximum amplitude of each current vs. time traces was recorded, averaged, and reported in the inset bar graph. Error bars were calculated using standard error the mean.

RESULTS AND DISCUSSION

Exposure to *In Vivo* Brain Environment Enhances Electrode Sensitivity. The brain environment is rich in proteins, ligands, and many other redox-active molecules that can interact with analytical probes. Such an interaction is thought to foul or poison the surface. Carbon is generally hydrophobic and more resistant to the fouling effects of biological agents than other common electrode materials.[45,46] Nonetheless, the carbon surface is altered when exposed to brain tissue. Detrimental interactions of biomolecules with carbon can be particularly problematic for low concentration measurements and/or analysis of rapidly fluctuating species, as is the case for *in vivo* analysis of serotonin neurotransmission. It is known that serotonin metabolites electropolymerize on CFMs and reduce the CFMs' sensitivity to serotonin.[22,31] This is an issue that we tackled in the past by pre-polymerizing a Nafion layer on the CFM under the rationale that Nafion, a cation exchange polymer, would repel negatively charged serotonin metabolites while preconcentrating serotonin cations.[22] The modification enables measurements of extremely low (approx. 10 nM) concentrations of evoked serotonin.[22,28] While our laboratory routinely makes these measurements, serotonin FSCV has not been adopted widely in the community because these signals are still very low. Thus, we began this work by addressing the Nafion coating since several Nafion (and other polymer) modification procedures have been updated since our first description.[22,35,36,47] We began by seeking to compare and contrast different CFM modification procedures in a bid to improve FSCV sensitivity to serotonin. Since there is a general notion that the sensitivity and/or response time of electrodes declines *in vivo,* as a starting point, we sought to confirm the detrimental effects of the *in vivo* environment on CFMs. We focused this section of the work on dopamine detection since the analysis of this molecule with FSCV is much better understood than serotonin analysis. Four-point calibrations were performed on 16 electrodes (Figure 1A,B).

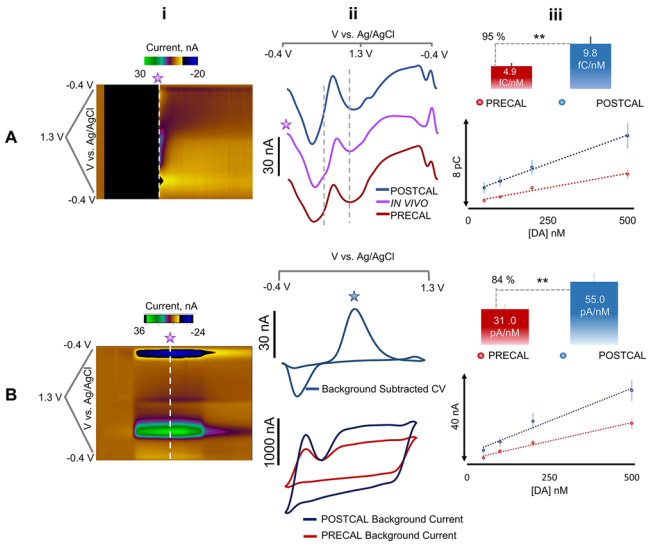

Figure 1. CFM sensitivity pre- and post *in vivo* experiments. (A) Pre- and post-calibration data from an *in vivo* experiment measuring dopamine in the mouse nucleus accumbens. (i) Representative *in vivo* FSCAV color plot and (ii) CVs in dopamine (500 nM), before (red), during (purple) and after (blue) *in vivo* measurements. (iii) Pre- (red) and post-calibration (blue). Inset bar graph depicts the increase in the post-calibration slope ($p < 0.01$). (B) Calibration data after an electrode was placed in the mouse dorsal striatum and cycled with the dopamine waveform for 2 h. (i) Representative FSCV color plot and (ii) CV in dopamine (500 nM) collected *via* FIA (above) along with the background signal during pre-calibration and post-calibration (below). (iii) Pre- and post-calibration plot. Inset bar graph depicts the increase in the post-calibration slope ($p < 0.01$). Error bars were calculated using standard error of the mean.

In Figure 1A, eight electrodes were calibrated in TRIS buffer before implantation into the nucleus accumbens of a mouse brain where extracellular dopamine was monitored for 2 h with FSCAV. Representative color plots and CVs from these experiments are shown in Figure 1Ai,ii, respectively. Interpretation of color plots can be found elsewhere;[48] briefly, these plots convey current vs voltage collected at 10 Hz against collection time, where current is given a false color. The calibration was repeated immediately following the *in vivo* experiment (calibrations are labeled PRECAL and POSTCAL in Figure 1Aiii). Contrary to the general view that the *in vivo* environment is detrimental to electrode sensitivity, we found that the electrode sensitivity significantly increased post *in vivo* implantation.

https://doi.org/10.1021/acs.analchem.0c04316
Anal. Chem. 2021, 93, 10762−10771

The slope of the calibration curve increased from 4.9 (±0.7) to 9.8 (±1.6) fC/nM (p = 0.001, paired t-test). This effect persisted when FSCV was used in a different brain region and calibrated in a different medium. In Figure 1B, CFMs were pre-calibrated, placed in the dorsal striatum of a mouse brain for 2 h to measure evoked dopamine release, and re-calibrated immediately thereafter in PBS. A representative color plot and CVs of the Faradaic and background signals are shown in Figure 1Bi,ii. The background current (mostly comprising capacitative current pre-background subtraction) substantially increases post *in vivo* implantation; an effect that persists with electrodes that have been electrochemically treated with glutamate only (Figure S2), showing that the surface chemistry of the electrode has changed. The pre- and post-calibration curves are in Figure 1Biii. In agreement with FSCAV results, the slope increased significantly in the post-calibration from 31.0 (±4.6) to 55.0 (±7.3) pA/nM (p = 0.004). These increases in sensitivity were not seen when the electrodes were tested in their respective control experiments in buffer alone (Figure S1).

These results contradict the general *status quo*, which is that electrodes lose sensitivity *in vivo*.[36,49,50] However, a previous study displayed similar results,[29] where the current response to acetaminophen after *in vivo* measurements was larger than before the experiment, and another where the response change to dopamine was insignificant.[51] There may be several factors to explain the contradiction such as experimental conditions, models and methods. Such differences may include electrode type (disk vs cylinder), waveform (1.0 V vs 1.3 V potential limit), pretreatment before post-calibration (overnight soaking in isopropyl alcohol vs no pretreatment post-calibration),[49] time *in vivo* (several weeks), which results in deterioration of the pseudo-Ag/AgCl reference electrode,[52] and the time after *in vivo* exposure and calibration (our calibration is immediately thereafter). Nonetheless, in our hands this effect is significant and persistent.

In sum, our results suggest that an unidentified aspect of the *in vivo* environment contributes to a surface alteration of carbon that improves the sensitivity of the electrode toward dopamine.

Analytical Response to Dopamine Is Improved with Glutamate Pretreatment. When identifying potential biological molecules that might interact with carbon, we identified glutamate, a neurotransmitter that is ubiquitous across brain regions. While it is generally accepted that glutamate does not offer analytical electroactivity, glutamate electropolymerization is well established in the literature with conventional, slow scan cyclic voltammetry.[40,42,53,54] In fact, electrochemical grafting of amines to carbon surfaces is well demonstrated *via* a radical-initiated C−N bond.[55−57] Applying an electrochemical potential not only drives bond formation between amine groups and carbon[56,57] but also facilitates electropolymerization of small amine-containing molecules like amino acids *via* a chain-like growth mechanism.[55] We thus hypothesized that, *in vivo*, the interaction of glutamate with CFMs may create a polymer layer that facilitates the increase in sensitivity observed in Figure 1. The rationale here is the structure of a potential PGA film, possessing an overall negative charge, would enhance the preconcentration of cations.

Figure 2 shows the first 3.5 s of a flow injection response of dopamine (1 μM) onto CFMs. Bare electrodes (1) served as controls and response to the dopamine injection was rapid, reaching the steady state (34.5 ± 3.8 nA) at 3.5 s (Figure 2A).

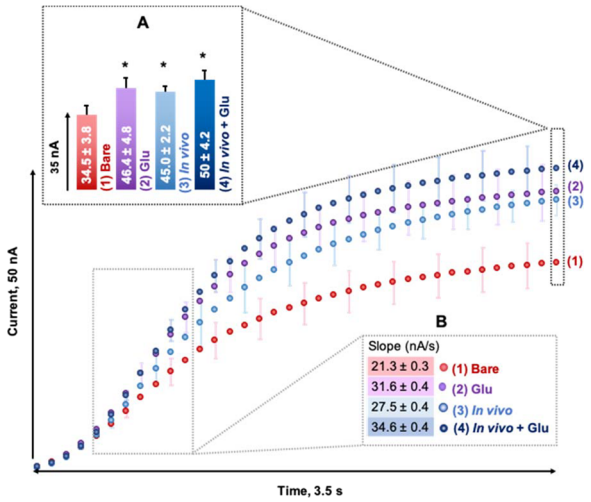

Figure 2. Analytical response of glutamate-treated and *in vivo* CFMs. FIA rise curves of the first 3.5 s of a 1 μM DA injection on four different CFMs: bare (1), glutamate in FIA buffer at 1 μM (2), *in vivo* (3), and *in vivo* + glutamate (4). Every third error bar is displayed. (A) Bar graph of the FIA response to 1 μM DA on each pretreated CFM (*p < 0.05). (B) Slope of the linear portion of the curve (0.4−1 s, R^2 > 0.99).

Electrodes pre-treated (*via* electrochemical cycling) with glutamate (2) prior to and during analysis at a concentration resembling ambient *in vivo* glutamate[58] had a significantly higher response than control (46.4 ± 4.8 nA, p = 0.05); the same held for CFMs that had been *in vivo* (3) (45 ± 2.2 nA, p = 0.03). The highest current was from electrodes that had been *in vivo* and were post-analyzed with glutamate in the FIA buffer (50 ± 4.2 nA, p = 0.02). A similar, significant increase in sensitivity is seen with FSCAV for electrodes before and after glutamate treatment (Figure S3).

A concern with modified electrodes is whether a diffusional barrier might induce temporal limitations in the response.[22] We tested whether any of these scenarios slowed down the FSCV response time *via* FIA in Figure 2B. In contrast to the expectation that modifications slow the response, we found by estimating the slope of the linear portion of the rise curve that all pre-treatments improved the speed of response ((3) 27.5 ± 0.4, (2) 31.6 ± 0.4, and (4) 34.6 ± 0.4 nA/s) with respect to the bare one ((1) 21.3 ± 0.3 nA/s). Combined, these data show that carbon fibers that have been *in vivo* or have been pretreated with glutamate display improved analytical response toward dopamine. We next explored the interaction of the carbon surface with glutamate.

Glutamate Electropolymerizes onto CFMs with FSCV. With conventional cyclic voltammetry, applying a high potential (>1.3 V) initiates grafting of the glutamate monomer to carbon followed by chain growth of the polymer.[39] Glutamate electropolymerization has not yet been explored with fast voltammetry; thus, we asked, does glutamate electropolymerization occur at the fast scan rates employed with FSCV?

We applied a waveform to the CFM with an intentionally wide potential window (−1.2 V to 1.3 V to −1.2 V at 400 V/s) to best capture any polymerization peaks. Using FIA, a rectangular pulse of glutamate (0.1 μM) was delivered to CFMs and the responses were averaged. A representative color plot and CV are displayed in Figure 3Ai,ii where the electropolymerization peak occurs at 1 V (denoted by the

https://doi.org/10.1021/acs.analchem.0c04316
Anal. Chem. 2021, 93, 10762−10771

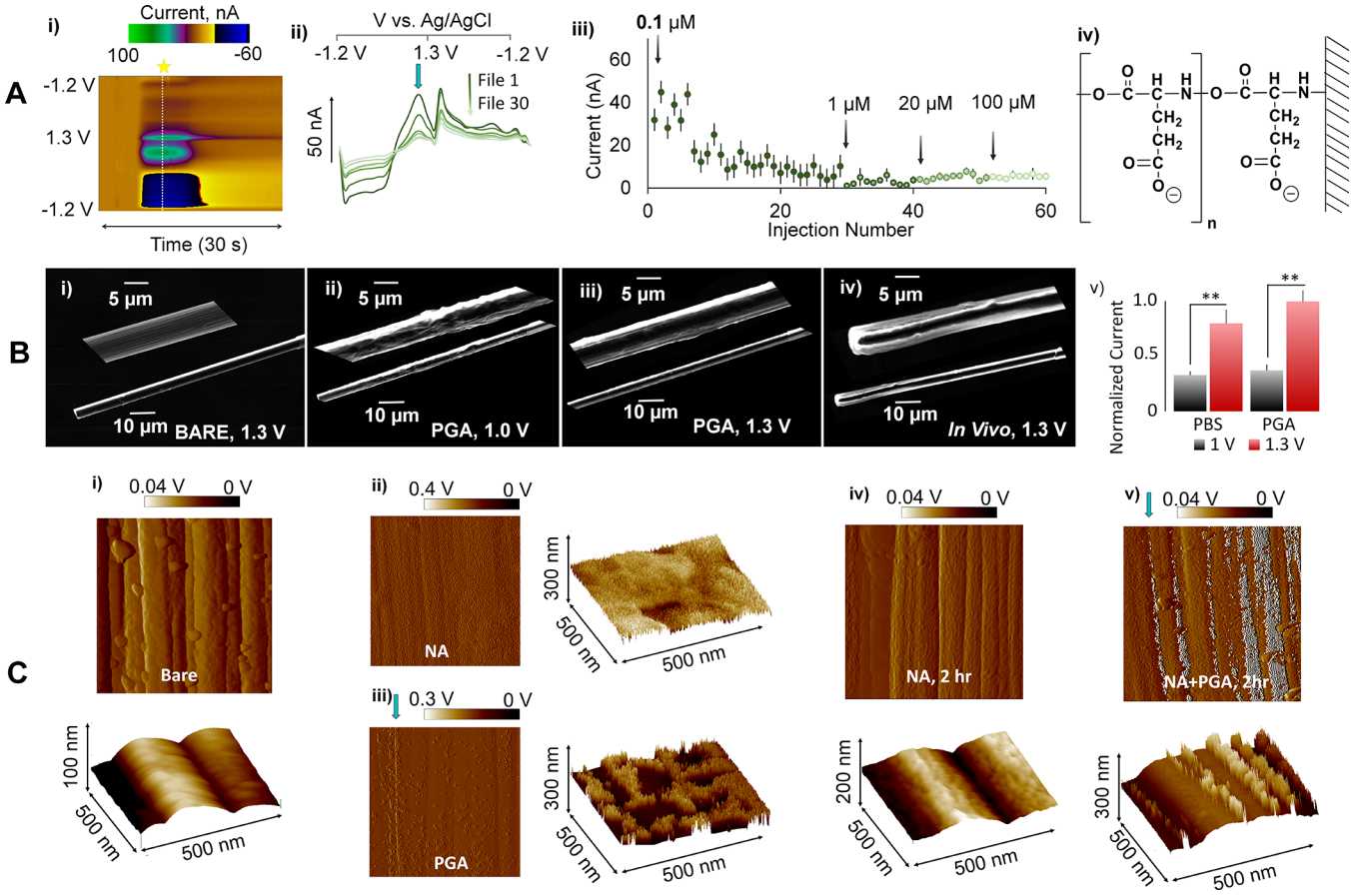

Figure 3. PGA electropolymerization and coatings on CFMs. (A) Glutamate electropolymerization at fast scan rates (i) Color plot from FIA injection of 0.1 μM glutamate. (ii) Every fourth CV of 0.1 μM glutamate is displayed. (iii) Varying concentrations (0.1, 1, 20, and 100 μM) of glutamate are measured by 60 successive injections *via* FIA. Error bars: standard error of the mean. (iv) Molecular structure PGA. (B) SEM images of CFMs: (i) bare, (ii) treated for 20 min (10 min 60 Hz, 10 min 10 Hz) in [10 mM] glutamate using the triangular DA waveform (to 1.0 V), (iii) using the extended dopamine waveform (to 1.3 V), and (iv) treated in brain tissue. (v) Bar graph comparing the normalized current response of CFMs to 1 μM DA, cycled at 1.0 V and 1.3 V in PBS and 1 μM glutamate. Statistics: *t*-test (**$p < 0.01$). (C) AFM images of CFMs modified by (i) surface activation with extended dopamine waveform (cycled 10 min 60 Hz, 10 min 10 Hz in PBS), (ii) electrodeposited Nafion and (iii) PGA coated with the extended dopamine waveform (10 min 60 Hz, 10 min 10 Hz in 1 μM glutamate). AFM images following exposure to the extended dopamine waveform for 2 h modified with (iv) electroplated Nafion and (v) Nafion with 1 μM glutamate added to the background buffer.

green arrow in Figure 3Aii). The first six injections in Figure 3Aiii reveal the polymerization peak, with an average current response of 36.7 ± 2.9 nA. Successive injections show that this peak diminishes over time (Figure 3Aii), decreasing to an average of 11.1 ± 1.0 nA or 30.2% ($p = 0.0002$) of the original amplitude. The polymerization peak is indistinguishable from the switching peak (an artifact of the FSCV technique) by scan 30. Even when the glutamate concentration was increased to 1, 20, and 100 μM, there was no significant change in amplitude. We believe the disappearance of this peak is due to fewer available sites for PGA attachment and chain length saturation. The structure of PGA on carbon is depicted in Figure 3Aiv. In previous studies describing PGA electropolymerization with conventional cyclic voltammetry, the free radical-initiated polymerization peak occurred at around +1.5 V.[39] Though the high potential is not within the potential window of our FSCV waveform, we hypothesized that adsorption of glutamate to CFMs creates enough thermodynamic favorability to initiate PGA formation. The polymerization peak at 1.0 V suggests that this process is dependent on the application of a positive potential above 1.0 V. PGA formation on CFMs with a fast-scan waveform that extends up to 1.3 V is an interesting finding since the application of 1.3 V is known to increase sensitivity to DA.[10] This effect has been attributed to overoxidation of the carbon surface, providing a fresh surface for the next analysis and for creating oxygen moieties on the surface that pre-concentrate the dopamine cation before analysis.[10,11] Here, we suggest that 1.3 V also facilitates the signal *via* PGA formation. Since electrochemical PGA formation onto the carbon surface is covalent, the over-oxidation process at 1.3V may be blocked at sites where PGA has grafted to the CFM.

Given voltammetric evidence of film formation, film deposition was verified and characterized *via* micro- and nanoimaging. PGA has been imaged on different carbon surfaces including glassy carbon,[40] carbon paste electrodes,[59] carbon nanotubes,[41,60,61] graphite,[62] and reduced graphene oxide[61,63] and other substrates such as Au nanoparticles;[64] however, there have been no reports of PGA deposition on CFMs. Here, we imaged CFM surfaces with SEM. In particular, we were interested in observing the effects of waveform limits (testing the importance of 1.3 V) on the CFM surface in the presence of glutamate. In Figure 3Bi, the CFM was cycled in PBS with a 1.3 V positive limit. The carbon surface appeared relatively smooth. In Figure 3Bii, the CFM was cycled in a glutamate-containing buffer with a positive

https://doi.org/10.1021/acs.analchem.0c04316
Anal. Chem. 2021, 93, 10762−10771

potential limit of 1.0 V; this waveform is not considered to overoxidize the carbon surface.[11,27,28] When treated in 1 μM glutamate, there were no visible deposits on the CFM (data not shown). This is because SEM does not have the resolving power to visualize the fine deposits of low glutamate concentrations (we visualize these with AFM in Figure 3B below). With 10 mM glutamate, significant deposits were visualized (Figure 3Bii). The large deposits indicate the presence of polymers. In Figure 3Biii, the electrode was in a glutamate-containing buffer and the positive potential limit of the waveform was increased to 1.3 V, a potential limit considered to etch the carbon surface. These electrodes appear to have a thinner deposition layer than the 1.0 V waveform (Figure 3Bii). In Figure 3Biv, the electrode was cycled *in vivo* for 20 minutes. There is a visible film on the electrode surface; such deposits have been previously seen after *in vivo* implantation, attributed to debris and biomaterials.[36,65]

The bar chart in Figure 3Bv compares the response to 1 μM dopamine before and after CFM treatment in 1 μM glutamate between the 1.0 and 1.3 V upper limit dopamine waveforms. In combination with the SEM images collected, the thinner apparent film corresponds to higher sensitivity to dopamine. This implies that having a positive limit of 1.0 V encourages a thicker layer of PGA, potentially creating a kinetic barrier. In contrast, the application of 1.3 V simultaneously etches the carbon as the polymer is deposited, such that the polymer is thin enough to act as a pre-concentration matrix and not as a barrier.

AFM is a useful tool for studying the morphology of conductive coatings on electrodes and could provide insights into how PGA is formed on electrodes *in vivo*. We compared different PGA deposition paradigms to Nafion (abbreviated to NA inFigure 3 and further figures) electrodeposition, which we have previously characterized in detail.[21−25,28] In Figure 3Ci, the distinct carbon striations are apparent on a bare CFM. After deposition of Nafion (Figure 3Cii) or PGA (Figure 3Ciii), the natural carbon striations are shallower and the surface is significantly roughened, as seen previously.[40,63,66,67] Other reports of PGA morphology with AFM on glassy carbon and reduced graphene oxide display similar surface features, however the PGA deposition was more homogeneous than we find.[40,63] When comparing the Nafion coating to the PGA coating, differences in morphology are clear. NA is uniformly deposited while PGA is deposited more sparsely with large patches of the surface devoid of the polymer. This is likely due to the inherent mechanistic differences between Nafion and PGA deposition: Nafion is electrostatically plated while PGA is polymerized from the monomer by covalently grafting to active sites on the carbon surface. In Figure 3Civ, theNafion-coated electrode was imaged after 2 hrs of electrochemical cycling and it is seen that the coating is degraded with time. Nafion-coated electrodes are commonly employed for biological analysis, and it has been thought that the Nafion-coating enhances the signal stability throughout an *in vivo* experiment,[22,32,35] a phenomenon difficult to reconcile with our finding here. Because at 1.3 V, the underlying carbon is etched away, a large portion of Nafion is removed; thus, it is interesting that Nafion-CFMs are still effective for *in vivo* experiments over several hours. This experiment, however, does not reflect the *in vivo* environment where there is a persistent, innate high concentration of glutamate. Thus, to better reflect the *in vivo* matrix, an Nafion-coated CFM was cycled for 2 hrs in the presence of ambient glutamate (Figure 3Cv). The deposits on this electrode appear more substantial. Of particular interest is the feature denoted by the blue arrow. Here, there appears to be heavy deposition along the vector of a single striation. This behavior implies that Nafion deposition is sparse within these ridges, leaving binding sites available for PGA initiation and that the deeper sections of carbon's striations are a more favorable surface for PGA deposition. We postulate that this is because there are more ridges or imperfection sites where the polymer can nucleate and grow. Nucleation and growth processes are dependent on surface imperfections and are described in great detail for metals.[68−70] This finding is not surprising since radical-initiated polymers are formed *via* chain growth (*vide supra*).[71−74] From this data, we suggest *in vivo* that PGA co-deposits on electrodes pretreated with Nafion, stabilizing, or even replacing the Nafion throughout an experiment.

PGA Facilitates Serotonin Detection. The investigations above with dopamine determined that PGA formation on carbon fibers increases electrode sensitivity and stability. We now asked whether these effects are maintained for serotonin. FSCV serotonin detection is fundamentally more challenging because of low evocable serotonin concentrations and high ambient concentrations of 5-HIAA; this metabolite also polymerizes on the electrode but serves to degrade the electrode sensitivity.[22,29−31] This is illustrated in Figure 4A

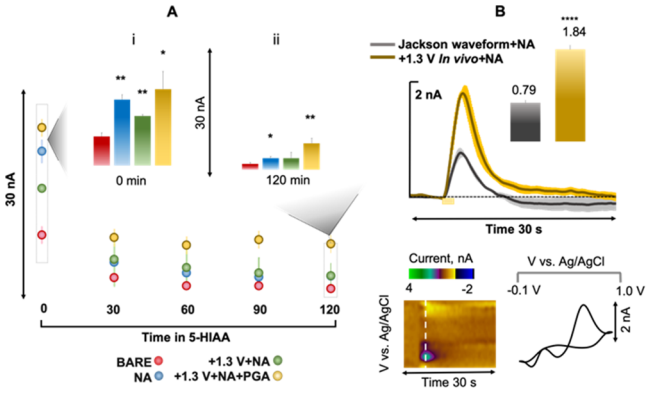

Figure 4. Serotonin responses with surface modifications with FIA and *in vivo*. (A) Time of exposure to 10 μM 5-HIAA (every 30 min for 2 h) vs current response (nA) is plotted of 100 nM serotonin, and surface modifications are compared: Bare (red, n = 3), NA (blue, n = 4), and Nafion-coated carbon fiber activation *via* exposure to an overoxidizing waveform (positive potential limit of 1.3 V, green n = 3) and PGA (yellow, n = 4). (i) Bar graphs of current response at initial (0 min) and final time point (120 min). (B) Current vs time traces of serotonin collected *in vivo* are averaged (n = 4) and compared: extended Jackson waveform pretreatment (yellow) vs. the Jackson waveform on NA electrodes (gray). Inset: bar graphs comparing the average amplitude of each treatment. Representative *in vivo* color plot and CV are shown below, where the oxidation and reduction peaks occur at 0.7 and 0 V, respectively. Statistics: t-test with respect to the bare electrode (**p < 0.01, *p < 0.05).

where bare electrodes (red markers) are utilized to measure serotonin (100 nM) with the standard Jackson waveform[75] giving a response of 7.4 ± 0.9 (red bar in the inset bar graph). When this electrode is cycled in a buffer containing 5-HIAA (5 μM), repeated injections of serotonin result in a significant loss of signals (1.3 ± 0.4 nA). While the initial response is greatly improved with Nafion modification (blue markers and blue bar in the bar graph) (16.8 ± 1.2 nA, p = 0.001 compared to bare), after 120 min of repeated serotonin injections in 5-HIAA, the

https://doi.org/10.1021/acs.analchem.0c04316
Anal. Chem. 2021, 93, 10762−10771

signal is significantly diminished (2.7 ± 0.4 nA, $p = 0.03$). This is consistent with the AFM study above that showed severe degradation to the Nafion layer with waveform application. The electrode response and stability can be substantially improved with the application of a pretreatment step whereby the Nafion-coated electrode is cycled in glutamate containing buffer with a 1.3 V upper limit on the Jackson waveform and then analyzed in a buffer that contains both 5-HIAA and glutamate with the 1.0 V waveform (yellow markers and trace; initial: 19.5 ± 4.6 nA, $p = 0.04$; final 6.4 ± 1.2 nA, $p = 0.01$). These results are consistent with our hypothesis above that glutamate serves to stabilize or replace Nafion when 1.3 V is applied. To show that this improvement in response is not a simple consequence of the 1.3 V upper limit creating more adsorption sites, the green markers and trace show that Nafion electrodes at cycled at 1.3 V without glutamate pretreatment or glutamate in the buffer do not have a significant effect on the response at the end of the experiment (initial: 12.6 ± 0.3 nA, $p = 0.003$; final 2.8 ± 1.3 nA, p = ns).

We thus followed the PGA paradigm to complete an *in vivo* experiment to test whether pretreating a Nafion electrode at 1.3 V in the brain would serve to increase sensitivity using the rationale that glutamate (and/or similar amino acids) facilitates the response. In Figure 4B, we measured serotonin in the CA2 region of the hippocampus of four mice with the Jackson waveform using a Nafion-coated electrode (black). Serotonin concentrations increase upon stimulation of the serotonin axons (denoted by the yellow bar under trace) and then clear rapidly after stimulation. We implemented an *in vivo* activation step (extending the Jackson waveform to a 1.3 V positive potential limit for 10 min at 60 Hz, 10 min at 10 Hz). The original Jackson waveform was restored for measurements. We observed a >2-fold increase in response as seen by the evoked release event (yellow; 0.79 ± 0.08 nA to 1.84 ± 0.11 nA, $p = 6 \times 10^{-5}$). A color plot and CV of this event (below) show the relative high integrity of the signal.

We do not believe that glutamate is the sole player here given the abundance of structurally analogous molecules in the brain (aspartate and lysine among others[76−78]). More likely, glutamate is part of an intricate network of molecules that polymerize in complex ways onto carbon and serve to draw equilibria that facilitate and impede the electrode's response. While we have long known about the detrimental effects of these molecules (such as 5-HIAA), here, we provide new evidence that glutamate's interactions with carbon are beneficial for dopamine and, importantly, serotonin detection, which was the initial aim of this project.

CONCLUSIONS

Carbon has been used for decades for biological analyses and is particularly applicable to neurotransmitter analysis in the CFM form. Much of the work with CFMs has been on dopamine detection, but our interests lie in improving serotonin detection at CFMs. We began this work by investigating the carbon surface under the assumption that exposure to the *in vivo* environment is detrimental to electrode sensitivity. In contrast to this assumption, we found that electrodes that had been exposed to the *in vivo* environment for up to 2 h were more sensitive to evoked and ambient dopamine. We postulated that high concentrations of innate glutamate *in vivo* serve to polymerize with a negative charge on CFMs and facilitate response to dopamine. We verified this polymerization electrochemically and characterized the mechanisms of deposition. Critically, we identified that the application of 1.3 V as an upper waveform limit is a key factor for increasing electrode sensitivity to dopamine and experimental stability by augmenting Nafion film integrity. Finally, we applied the knowledge gained from these dopamine data sets to an *in vivo* serotonin experiment where we were able to induce a 2-fold increase in response to serotonin. We present not only the novel finding that innate aspects of the *in vivo* environment are auspicious for dopamine and serotonin detection *via* carbon, but also offer an improved FSCV serotonin detection paradigm.

ASSOCIATED CONTENT

Supporting Information

The Supporting Information is available free of charge at https://pubs.acs.org/doi/10.1021/acs.analchem.0c04316.

Pre- and post-calibration effects; pre- and post-glutamate polymerization background current; and pre- and post-glutamate polymerization effects—FSCAV analysis (PDF)

AUTHOR INFORMATION

Corresponding Author

Parastoo Hashemi − *Department of Chemistry and Biochemistry, University of South Carolina, Columbia, South Carolina 29208, United States; Department of Bioengineering, Imperial College, London SW7 2AZ, UK;* orcid.org/0000-0002-0180-767X; Email: phashemi@imperial.ac.uk

Authors

Jordan Holmes − *Department of Chemistry and Biochemistry, University of South Carolina, Columbia, South Carolina 29208, United States*

Colby E. Witt − *Department of Chemistry and Biochemistry, University of South Carolina, Columbia, South Carolina 29208, United States*

Deanna Keen − *Department of Chemistry and Biochemistry, University of South Carolina, Columbia, South Carolina 29208, United States*

Anna Marie Buchanan − *Department of Chemistry and Biochemistry, University of South Carolina, Columbia, South Carolina 29208, United States; Department of Pharmacology, Physiology, & Neuroscience, University of South Carolina SOM, Columbia, South Carolina 29209, United States*

Lauren Batey − *Department of Chemistry and Biochemistry, University of South Carolina, Columbia, South Carolina 29208, United States; Department of Bioengineering, Imperial College, London SW7 2AZ, UK*

Melinda Hersey − *Department of Chemistry and Biochemistry, University of South Carolina, Columbia, South Carolina 29208, United States; Department of Pharmacology, Physiology, & Neuroscience, University of South Carolina SOM, Columbia, South Carolina 29209, United States*

Complete contact information is available at: https://pubs.acs.org/10.1021/acs.analchem.0c04316

Author Contributions

The manuscript was written through contributions of all authors. All authors have given approval to the final version of the manuscript.

Notes

The authors declare no competing financial interest.

■ ACKNOWLEDGMENTS

We would like to thank Yangguang Ou and Sergio Mena for their assistance with modeling software and statistical analysis as well as Shane Berger and Alyssa West for assisting with *in vivo* experiments. Additionally, we acknowledge Asif Khan, Mohammad Kamal Hussain, Mikhail Gaevski, and Pavithra Pathirathna for helping to optimize AFM imaging protocols for CFMs. Finally, we thank Yangguang Ou, Shane Berger, Solene Dietsch, and Melissa Hexter for helpful discussions and editing the manuscript. NSF CAREER Award CHE-1654111 (P.H.) funded this work.

■ REFERENCES

(1) Hersey, M.; Berger, S. N.; Holmes, J.; West, A.; Hashemi, P. *Anal. Chem.* **2019**, *91*, 27−43.
(2) Schroeder, V.; Savagatrup, S.; He, M.; Lin, S.; Swager, T. M. *Chem. Rev.* **2019**, *119*, 599−663.
(3) Kurbanoglu, S.; Ozkan, S. A. *J. Pharm. Biomed. Anal.* **2018**, *147*, 439−457.
(4) Liu, Y.; Wang, H.; Zhao, W.; Zhang, M.; Qin, H.; Xie, Y. *Sensors* **2018**, *18*, 645.
(5) Roberts, J. G.; Sombers, L. A. *Anal. Chem.* **2018**, *90*, 490−504.
(6) Rodeberg, N. T.; Sandberg, S. G.; Johnson, J. A.; Phillips, P. E. M.; Wightman, R. M. *ACS Chem. Neurosci.* **2017**, *8*, 221−234.
(7) Bergstrom, B. P.; Sanberg, S. G.; Andersson, M.; Mithyantha, J.; Carroll, F. I.; Garris, P. A. *Neuroscience* **2011**, *193*, 310−322.
(8) Addy, N. A.; Daberkow, D. P.; Ford, J. N.; Garris, P. A.; Wightman, R. M. *J. Neurophysiol.* **2010**, *104*, 922−931.
(9) Owesson-White, C. A.; Ariansen, J.; Stuber, G. D.; Cleaveland, N. A.; Cheer, J. F.; Mark Wightman, R.; Carelli, R. M. *Eur. J. Neurosci.* **2009**, *30*, 1117−1127.
(10) Heien, M. L. A. V.; Phillips, P. E. M.; Stuber, G. D.; Seipel, A. T.; Wightman, R. M. *Analyst* **2003**, *128*, 1413−1419.
(11) Takmakov, P.; Zachek, M. K.; Keithley, R. B.; Walsh, P. L.; Donley, C.; McCarty, G. S.; Wightman, R. M. *Anal. Chem.* **2010**, *82*, 2020−2028.
(12) Bath, B. D.; Michael, D. J.; Trafton, B. J.; Joseph, J. D.; Runnels, P. L.; Wightman, R. M. *Anal. Chem.* **2000**, *72*, 5994−6002.
(13) DuVall, S. H.; McCreery, R. L. *J. Am. Chem. Soc.* **2000**, *122*, 6759−6764.
(14) DuVall, S. H.; McCreery, R. L. *Anal. Chem.* **1999**, *71*, 4594−4602.
(15) Cryan, M. T.; Ross, A. E. *Analyst* **2018**, *144*, 249−257.
(16) Samaranayake, S.; Abdalla, A.; Robke, R.; Wood, K. M.; Zeqja, A.; Hashemi, P. *Analyst* **2015**, *140*, 3759−3765.
(17) Swamy, B. E. K.; Venton, B. J. *Anal. Chem.* **2007**, *79*, 744−750.
(18) Sanford, A. L.; Morton, S. W.; Whitehouse, K. L.; Oara, H. M.; Lugo-Morales, L. Z.; Roberts, J. G.; Sombers, L. A. *Anal. Chem.* **2010**, *82*, 5205−5210.
(19) Pathirathna, P.; Yang, Y.; Forzley, K.; McElmurry, S. P.; Hashemi, P. *Anal. Chem.* **2012**, *84*, 6298−6302.
(20) Yang, Y.; Pathirathna, P.; Siriwardhane, T.; McElmurry, S. P.; Hashemi, P. *Anal. Chem.* **2013**, *85*, 7535−7541.
(21) Wood, K. M.; Hashemi, P. *ACS Chem. Neurosci.* **2013**, *4*, 715−720.
(22) Hashemi, P.; Dankoski, E. C.; Petrovic, J.; Keithley, R. B.; Wightman, R. M. *Anal. Chem.* **2009**, *81*, 9462−9471.
(23) West, A.; Best, J.; Abdalla, A.; Nijhout, H. F.; Reed, M.; Hashemi, P. *Neurochem. Int.* **2019**, *123*, 50−58.
(24) Saylor, R. A.; Hersey, M.; West, A.; Buchanan, A. M.; Berger, S. N.; Nijhout, H. F.; Reed, M. C.; Best, J.; Hashemi, P. *Front Neurosci.* **2019**, *13*, 362.
(25) Abdalla, A.; West, A.; Jin, Y.; Saylor, R.; Qiang, B.; Peña, E.; Linden, D. J.; Nijhout, H. F.; Reed, M. C.; Best, J.; Hashemi, P. *J. Neurochem.* **2020**, *153*, 33.
(26) Abdalla, A.; Atcherley, C. W.; Pathirathna, P.; Samaranayake, S.; Qiang, B. D.; Pena, E.; Morgan, S. L.; Heien, M. L.; Hashemi, P. *Anal. Chem.* **2017**, *89*, 9703−9711.
(27) Wood, K. M.; Zeqja, A.; Nijhout, H. F.; Reed, M. C.; Best, J.; Hashemi, P. *J. Neurochem.* **2014**, *130*, 351−359.
(28) Hashemi, P.; Dankoski, E. C.; Lama, R.; Wood, K. M.; Takmakov, P.; Wightman, R. M. *Proc. Natl. Acad. Sci. U. S. A.* **2012**, *109*, 11510−11515.
(29) Logman, M. J.; Budygin, E. A.; Gainetdinov, R. R.; Wightman, R. M. *J. Neurosci. Methods* **2000**, *95*, 95−102.
(30) Dankoski, E. C.; Wightman, R. M. *Front Integr. Neurosci.* **2013**, *7*, 44.
(31) Singh, Y. S.; Sawarynski, L. E.; Dabiri, P. D.; Choi, W. R.; Andrews, A. M. *Anal. Chem.* **2011**, *83*, 6658−6666.
(32) Gerhardt, G. A.; Oke, A. F.; Nagy, G.; Moghaddam, B.; Adams, R. N. *Brain Res.* **1984**, *290*, 390−395.
(33) Rice, M. E.; Nicholson, C. *Anal. Chem.* **1989**, *61*, 1805−1810.
(34) Cahill, P. S.; Walker, Q. D.; Finnegan, J. M.; Mickelson, G. E.; Travis, E. R.; Wightman, R. M. *Anal. Chem.* **1996**, *68*, 3180−3186.
(35) Ross, A. E.; Venton, B. J. *Analyst* **2012**, *137*, 3045−3051.
(36) Vreeland, R. F.; Atcherley, C. W.; Russell, W. S.; Xie, J. Y.; Lu, D.; Laude, N. D.; Porreca, F.; Heien, M. L. *Anal. Chem.* **2015**, *87*, 2600−2607.
(37) Demuru, S.; Deligianni, H. *J. Electrochem. Soc.* **2017**, *164*, G129−G138.
(38) Taylor, I. M.; Robbins, E. M.; Catt, K. A.; Cody, P. A.; Happe, C. L.; Cui, X. T. *Biosens. Bioelectron.* **2017**, *89*, 400−410.
(39) Yu, A. M.; Chen, H. Y. *Anal. Lett.* **1997**, *30*, 599−607.
(40) Santos, D. P.; Zanoni, M. V. B.; Bergamini, M. F.; Chiorcea-Paquim, A. M.; Diculescu, V. C.; Brett, A. M. O. *Electrochim. Acta* **2008**, *53*, 3991−4000.
(41) Liu, X.; Luo, L.; Ding, Y.; Ye, D. *Bioelectrochemistry* **2011**, *82*, 38−45.
(42) Zhang, L.; Lin, X. *Analyst* **2001**, *126*, 367−370.
(43) Atcherley, C. W.; Laude, N. D.; Parent, K. L.; Heien, M. L. *Langmuir* **2013**, *29*, 14885−14892.
(44) Atcherley, C. W.; Wood, K. M.; Parent, K. L.; Hashemi, P.; Heien, M. L. *Chem. Commun.* **2015**, *51*, 2235−2238.
(45) Harreither, W.; Trouillon, R.; Poulin, P.; Neri, W.; Ewing, A. G.; Safina, G. *Anal. Chem.* **2013**, *85*, 7447−7453.
(46) Trouillon, R.; O'Hare, D. *Electrochim. Acta* **2010**, *55*, 6586−6595.
(47) Qi, L.; Thomas, E.; White, S. H.; Smith, S. K.; Lee, C. A.; Wilson, L. R.; Sombers, L. A. *Anal. Chem.* **2016**, *88*, 8129−8136.
(48) Michael, D.; Travis, E. R.; Wightman, R. M. *Anal. Chem.* **1998**, *70*, 586A−592A.
(49) Roberts, J. G.; Toups, J. V.; Eyualem, E.; McCarty, G. S.; Sombers, L. A. *Anal. Chem.* **2013**, *85*, 11568−11575.
(50) Ewing, A. G.; Dayton, M. A.; Wightman, R. M. *Anal. Chem.* **1981**, *53*, 1842−1847.
(51) Ewing, A. G.; Wightman, R. M.; Dayton, M. A. *Brain Res.* **1982**, *249*, 361−370.
(52) Seaton, B. T.; Hill, D. F.; Cowen, S. L.; Heien, M. L. *Anal. Chem.* **2020**, *92*, 6334−6340.
(53) Wang, W.; Li, S.; Zhang, G.; He, J.; Ma, Z. *Int. J. Electrochem. Sci.* **2017**, *12*, 10791−10799.
(54) Zhou, X.; Zheng, X.; Lv, R.; Kong, D.; Li, Q. *Electrochim. Acta* **2013**, *107*, 164−169.
(55) Adenier, A.; Chehimi, M. M.; Gallardo, I.; Pinson, J.; Vila, N. *Langmuir* **2004**, *20*, 8243−8253.
(56) Barbier, B.; Pinson, J.; Desarmot, G.; Sanchez, M. *J. Electrochem. Soc.* **1990**, *137*, 1757−1764.

https://doi.org/10.1021/acs.analchem.0c04316
Anal. Chem. 2021, 93, 10762−10771

(57) Deinhammer, R. S.; Ho, M.; Anderegg, J. W.; Porter, M. D. *Langmuir* **1994**, *10*, 1306−1313.
(58) Moussawi, K.; Riegel, A.; Nair, S.; Kalivas, P. W. *Front. Syst. Neurosci.* **2011**, *5*, 94.
(59) Ganesh, P. S.; Swamy, B. E. K. *J. Electroanal. Chem.* **2015**, *752*, 17−24.
(60) Bui, M. P. N.; Li, C. A.; Seong, G. H. *BioChip J.* **2012**, *6*, 149−156.
(61) Deng, K.; Liu, X.; Li, C.; Hou, Z.; Huang, H. *Anal. Methods* **2017**, *9*, 5509−5517.
(62) Raj, M.; Goyal, R. N. *Sens. Actuators, B* **2017**, *250*, 552−562.
(63) Feminus, J. J.; Manikandan, R.; Narayanan, S. S.; Deepa, P. N. *J Chem Sci* **2019**, *131*, 11.
(64) Karaboga, M. N. S.; Sezginturk, M. K. *Analyst* **2019**, *144*, 611−621.
(65) Shepherd, R. K.; Murray, M. T.; Houghton, M. E.; Clark, G. M. *Biomaterials* **1985**, *6*, 237−242.
(66) Hiesgen, R.; Aleksandrova, E.; Meichsner, G.; Wehl, I.; Roduner, E.; Friedrich, K. A. *Electrochim. Acta* **2009**, *55*, 423−429.
(67) Ou, L.-B.; Liu, Y.-N.; Wang, J.; Zhang, L. *J. Nanosci. Nanotechnol.* **2009**, *9*, 6614−6619.
(68) Simm, A. O.; Ji, X.; Banks, C. E.; Hyde, M. E.; Compton, R. G. *ChemPhysChem* **2006**, *7*, 704−709.
(69) Hyde, M. E.; Compton, R. G. *J. Electroanal. Chem.* **2003**, *549*, 1−12.
(70) Wildgoose, G. G.; Banks, C. E.; Compton, R. G. *Small* **2006**, *2*, 182−193.
(71) Hwang, B. J.; Santhanam, R.; Lin, Y. L. *J. Electrochem. Soc.* **2000**, *147*, 2252−2257.
(72) Soto, J. P.; Díaz, F. R.; Del Valle, M. A.; Vélez, J. H.; East, G. A. *Appl. Surf. Sci.* **2008**, *254*, 3489−3496.
(73) Qiu, Y. J.; Reynolds, J. R. *J. Polym. Sci.,Part A: Polym. Chem.* **1992**, *30*, 1315−1325.
(74) Koizumi, Y.; Shida, N.; Ohira, M.; Nishiyama, H.; Tomita, I.; Inagi, S. *Nat. Commun.* **2016**, *7*, 1.
(75) Jackson, B. P.; Dietz, S. M.; Wightman, R. M. *Anal. Chem.* **1995**, *67*, 1115−1120.
(76) Robinson, N.; Williams, C. B. *Clin. Chim. Acta* **1965**, *12*, 311.
(77) Hallen, A.; Jamie, J. F.; Cooper, A. J. L. *Amino Acids* **2013**, *45*, 1249−1272.
(78) Ota, N.; Shi, T.; Sweedler, J. V. *Amino Acids* **2012**, *43*, 1873−1886.

https://doi.org/10.1021/acs.analchem.0c04316
Anal. Chem. 2021, 93, 10762−10771